

Supporting Information

Zwitterionic Ring-Opening Polymerization: Models for Kinetics of Cyclic Poly(caprolactone) Synthesis

Hayley A. Brown¹, Silei Xiong², Grigori A. Medvedev², Young A. Chang¹, Mahdi M. Abu-Omar³, James M. Caruthers², Robert M. Waymouth*,¹

¹ Department of Chemistry, Stanford University, Mudd Building, 333 Campus Drive, Stanford, California 94305, United States

² School of Chemical Engineering, Purdue University, Forney Hall of Chemical Engineering, 480 Stadium Mall Drive, West Lafayette, Indiana 47907, United States

³ Brown Laboratory, Department of Chemistry, Purdue University, 560 Oval Drive, West Lafayette, Indiana 47907, United States

* Corresponding author. E-mail: waymouth@stanford.edu

Contents

Experimental procedures.....	2
General Considerations	2
Materials.....	2
Representative polymerization of ϵ -Caprolactone with 1, 3,4,5-tetramethyl-imidazol-2-ylidene	3
Representative procedure for preparation of linear poly(ϵ -caprolactone).....	3
Representative procedure for preparation of linear poly(ϵ -caprolactone).....	3
Mark-Houwink plot of cyclic and linear PCL.....	4
Stochastic simulations using DMC.....	5
Additional Simulations.....	6
References.....	8

Experimental procedures

General Considerations.

All reactions and polymerizations were performed in a drybox or with Schlenk techniques under nitrogen. ^1H nuclear magnetic resonance (NMR) spectra were recorded at room temperature on either a 400 MHz or 500 MHz spectrometer, with shifts reported in parts per million downfield from tetramethylsilane and referenced to the residual solvent peak. Gel permeation chromatography (GPC) was performed in tetrahydrofuran (THF) at a flow rate of 1.0 mL/min on a Waters chromatograph equipped with four 5 μm Waters columns (300 mm x 7.7 mm) connected in series. The Viscotek S3580 refractive index detector and Viscotek GPCmax autosampler were employed. The system with a triple detection system (Viscotek, Houston, TX) including a light scattering detector and viscometer was calibrated using monodisperse polystyrene standards (Polymer Laboratories). The right-angle light scattering (RALS) method was used to determine absolute molecular weights of polymers. Correction for any angular dissymmetry factor in the RALS data was performed in the TriSEC software using the viscometer signal. The angular dissymmetry correction is negligible because the polymers studied are relatively small compared to the laser wavelength (610 nm). The polymer solution (ca. 10 mg/mL) was prepared by dissolving the polymer in THF.

Materials.

Toluene was distilled from sodium/benzophenone and degassed three times via freeze-pump-thaw cycles. ϵ -Caprolactone (CL) was purchased from Sigma-Aldrich and distilled from calcium hydride twice. Anhydrous methanol was purchased from Sigma-Aldrich and used as received. 4-Nitrophenol was purchased from Fluka and purified by recrystallization from toluene and sublimation. 1,3-bis(2,4,6-trimethylphenyl)imidazole-2-ylidene (IMes, **1**), 1,3,4,5-tetramethyl-imidazol-2-ylidene (**2**), 1,3-diethyl-4,5-dimethylimidazol-2-ylidene (**3**), and 1,3-diisopropyl-4,5-dimethylimidazol-2-ylidene (**4**), and were prepared according to the literature procedures.^{1,2} Linear PCL was prepared according to literature procedure.³

Representative procedure for kinetic monitoring of polymerization of cyclic ϵ -Caprolactone with 1,3,4,5-tetramethyl-imidazol-2-ylidene in J, (2)

Liquid CL monomer (0.1433 g, 1.257 mmol) was weighed into a vial in the glovebox and dissolved in d_8 -toluene (1.00 mL). This solution was placed in a J. Young NMR tube, sealed, and used to lock and shim the NMR used for acquisition (300 MHz). The NMR tube was returned to the glovebox and NHC **2** was added as a solution in d_8 -toluene (1.575 mg in 0.25 mL toluene from stock solution, 0.0127mmol). The reaction was monitored by 1 H NMR overnight.

Representative procedure for preparation of cyclic poly(ϵ -caprolactone).

To a stirred solution of ϵ -caprolactone (0.2915g, 2.554mmol) in toluene (1.83mL) was added a solution of **NHC 2** (3.17mg, 0.0255mmol) in toluene (0.72 mL, from a stock solution) at room temperature. The resulting solution was stirred at room temperature for 120 min. 4-Nitrophenol (20mg, 0.144mmol) was added and stirring was continued for 1 h. Conversion was determined by 1 H NMR spectroscopy (97% conversion). The polymer was purified by precipitation from methanol and analyzed by 1 H NMR spectroscopy and GPC. 1 H NMR ($CDCl_3$, 500 MHz): δ 1.32-1.44 (m, $CH_2CH_2CH_2$), δ 1.58-1.70 (m, $CH_2CH_2CH_2$), δ 2.26-2.34 (t, $OC(=O)CH_2$), δ 4.01-4.09 (t, $C(=O)OCH_2$) ppm; GPC (THF) M_n = 105 kg/mol, PDI = 1.73 (conventional PS calibration).

Representative procedure for preparation of linear poly(ϵ -caprolactone).

To a stirred solution of ϵ -caprolactone (1.14 g, 9.99 mmol) in THF (8.7 mL) was added a solution of $Et_2Al(OMe)$ (1.14 mg, 0.00982 mmol) in THF (0.19 mL) (from a stock solution) at room temperature. The resulting solution was stirred at room temperature for 8 h and the reaction was quenched by adding four drops of acetic acid. Conversion was determined by 1 H NMR spectroscopy (90% conversion). The polymer was purified by precipitation from methanol and analyzed by 1 H NMR spectroscopy and GPC. 1 H NMR ($CDCl_3$, 500 MHz): δ 1.32-1.44 (m, $CH_2CH_2CH_2$), δ 1.58-1.70 (m, $CH_2CH_2CH_2$), δ 2.26-2.34 (t, $OC(=O)CH_2$), δ 3.64 (m, CH_2CH_2OH), δ 3.66 (s, $C(=O)OCH_3$), δ 4.01-4.09 (t, $C(=O)OCH_2$) ppm; GPC (THF) M_n = 140 kg/mol, PDI = 1.54 (conventional PS calibration)

Mark-Houwink plot of cyclic and linear PCL

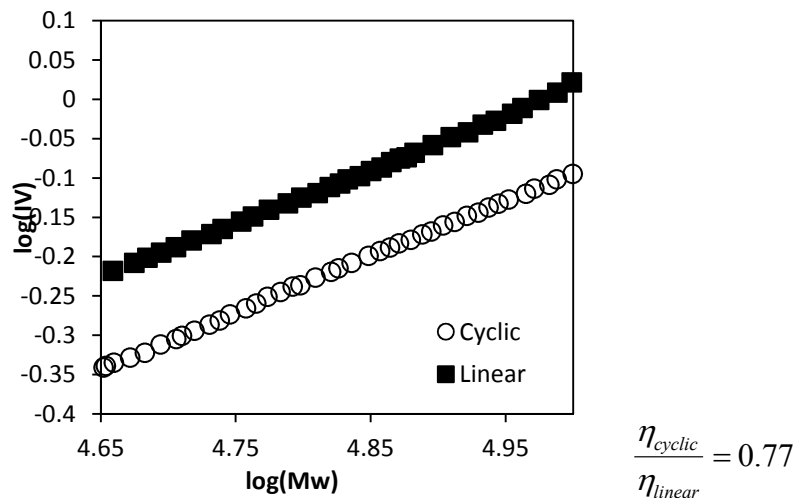


Figure S1. Mark Houwink plot of intrinsic viscosity vs. Mw of linear and cyclic PCL.

Table S1. Evolution of Conversion and Molecular weight vs. Time for the zwitterionic ring-opening polymerization of CL with carbene **2** at 25°C

Sample	Time (min)	Conv. (%)	Mn (Da)	Mw/Mn
YC-2-19A	10	24	36,700	1.15
YC-2-19B	20	32	54,300	1.52
YC-2-19C	30	56	58,100	1.77
YC-2-19D	60	76	76,900	1.65
YC-2-19E	120	98	106,000	1.73
HB-8-14A	30	35	84,700	1.60
HB-8-14B	60	64	77,500	2.60
HB-8-14C	90	84	160,000	2.00
HB-8-14D	120	89	88,600	2.10
HB-8-14E	180	95	79,800	5.15
HB-8-15A	30	27	59,900	1.31
HB-8-15B	60	56	67,000	1.45
HB-8-15C	90	70	101,000	2.04
HB-8-15E	180	94	59,400	7.69

Stochastic simulations using DMC

For a given reaction mechanism the concentrations of all the species as a function of time are obtained in this work using the Dynamic Monte Carlo (DMC) method⁴. It should be noted that the more traditional analysis method⁵ is based on solving a set of coupled ordinary differential equations (ODE)s for species concentrations. Although adequate in most cases, the traditional method fails when the number of reacting species is combinatorially intractable. As will be shown below such a situation arises when attack of a growing chain end on dormant cyclic chains or other growing chains is considered, where for example a growing chain of length n (i.e. consisting of n repeat units) can react with another chain of length m resulting in creation of the two new chains of lengths n' and m' (where $n+m=n'+m'$).

The implementation of the DMC method here is based on the Gillespie's algorithm⁴ for which an original computer code has been created.⁵ We model a finite set of molecules contained in a control volume V . Hence the initial number of molecules of species i , X_{i0} can be calculated via

$$X_{i0} = [x_i]_0 V$$

, where $[x_i]_0$ is the initial concentration of each species in an experimental run. The probability that the reaction will occur given that the collision of the reactant molecules has happened is characterized by reaction parameter c_μ . The conversion between the reaction parameter c_μ and macroscopic reaction rate constant k_μ is given by

$$k_\mu = c_\mu$$

for unimolecular reaction, and

$$k_\mu = V c_\mu$$

for bimolecular reactions between different molecules. The number of reactant combinations for a particular reaction is denoted as h_μ . h_μ for every elementary step (shown in the main text) are listed below:

(1) initiation (Scheme 2):	$h_1 = X_I X_M$
(2) reverse initiation (Scheme 2):	$h_2 = X_{Z_1}$
(3) propagation (Scheme 2):	$h_3 = X_M \left(\sum_n X_{Z_n} \right)$
(4) cyclization (Eq. 1):	$h_4 = \sum_n X_{Z_n}$

(5) carbene attack (Eqs. 2 and 3):

$$h_5 = X_I \left(\sum_n nX_{Z_n} + \sum_n nX_{C_n} \right)$$

(6) back-biting (Eq. 4):

$$h_6 = \sum_n X_{Z_n}$$

(7) intermolecular chain transfer
(Eqs. 5 and 6):

$$h_7 = \left(\sum_m X_{Z_m} \right) \left(\sum_n nX_{Z_n} + \sum_n nX_{C_n} \right)$$

where X_i is the number of molecules of species i , e.g., X_I is the number of molecules of carbene initiator I, X_{Z_n} is the number of molecules of growing zwitterion Z_n , and nX_{Z_n} is the number of repeat units in Z_n .

The maximum chain length observed in the experiment is approximately 10^4 . The choice of the control volume must be such that there is initially enough monomer to at least in principle form chains of such length, in practice the control volume here contains 10^5 molecules which was verified to give a good compromise between the numerical efficiency and accuracy of the MWD prediction. Each run containing 10^5 molecules is repeated 10^3 times in order to get relatively smooth MWD curves, thus the total number of simulated molecules is 10^8 . In the end numbers of molecules are converted back to concentrations according to:

$$[x_i] = \frac{\sum_{\text{repeats}} X_i}{V \cdot N_{\text{repeat}}}$$

Additional Simulations.

Inclusion of these reactions into Model III will result in changes in the optimized values of the rate constants present in Table 4. To access the extent to which cyclization reaction (Eq 1) may be present, we do the following: (1) the cyclization step is added to Model III. As seen in Figure S2a, this results in an effective deactivation of zwitterions via the mechanism described in Model II section. Even at the rate constant value of $k_c = 0.001 \text{ min}^{-1}$, the deviation of the model prediction from the data is beyond the experimental uncertainty for the lowest concentration of initiator and monomer (run 5). At the higher value of k_c (e.g., $k_c = 0.05 \text{ min}^{-1}$, dashed in Figure S2a), the discrepancy becomes even more dramatic. (2) If both cyclization and attack of the carbene on growing zwitterions or macrocycles, i.e., entire Model II is combined with Model III, the performance of the model improves; however, as illustrated in Figure S2bc, only relatively

small amount of k_c and k_{ca} reactions can be accommodated. Specifically, at the values of $k_c = 0.007 \text{ min}^{-1}$, $k_{ca} = 0.001 \text{ M}^{-1} \text{ min}^{-1}$, the rate of monomer consumption at the highest $[I]_0$ (run 1, red curve) is too fast compared to the data and the rate of monomer consumption at the lowest $[I]_0$ (run 5, green curve) is too slow. Larger k_c values result in even bigger deviations. Note that in the presence of cyclization reaction, the rate of back-biting (k_{bb}) had to be adjusted to preserve the fit to the MWD. The estimate for the rate of cyclization obtained here is an upper bound which can be made tighter with more experimental data becoming available. Another conclusion is that the optimized set of rate constants for the Model III is only slightly affected (k_{bb} was changed by 10%).

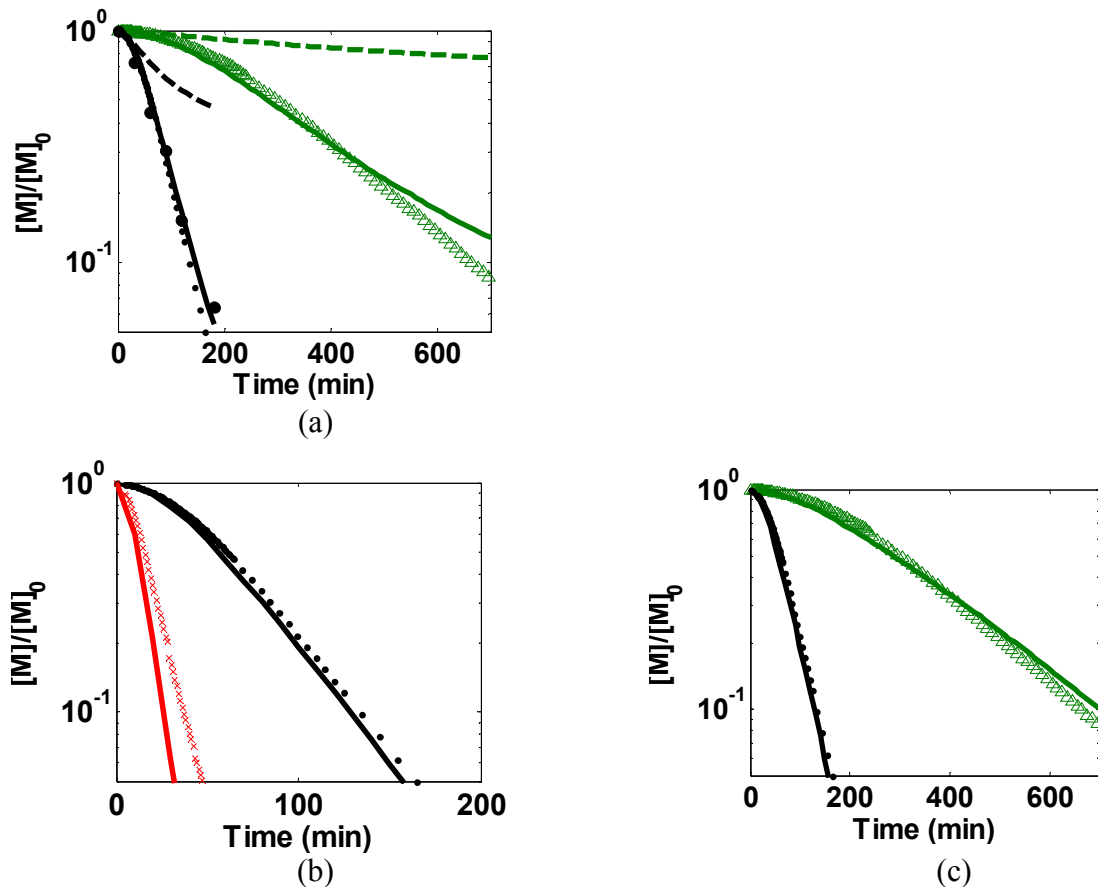


Figure S2. Simulation results of monomer consumption data of run **1** (red), **3a** (black), and **5** (green) ($[I]_0 = 0.05, 0.01, 0.006 \text{ M}$, respectively). Symbols are data, lines are fits. Rate constants for optimized Model III (Table 4 in the paper) were used unless mentioned: (a) Model III with added step of cyclization (eq 1 of text) dashed lines: $k_c = 0.05 \text{ min}^{-1}$, solid lines: $k_c = 0.001 \text{ min}^{-1}$, and Xcarbene = 30% for both. (b, c) Model III with added steps of cyclization (eq 1) and chain attack (eqs 2 and 3) $k_c = 0.007 \text{ min}^{-1}$, $k_{ca} = 0.001 \text{ M}^{-1} \text{ min}^{-1}$, for Xcarbene = 40%. (b) and (c) use the same set of rate constants but are plotted in different time scale.

References

- (1) Arduengo, I., AJ; Dias, H.; Harlow, R. *J. Am. Chem. Soc.* **1992**, *114*, 5530-5534.
- (2) Kuhn, N.; Kratz, T. *Synthesis-Stuttgart* **1993**, 561-562.
- (3) Storey, R. F.; Herring, K. R.; Hoffman, D. C. *J. Polym. Sci., Part A: Polym. Chem.* **1991**, *29*, 1759.
- (4) Gillespie, D. T. *J. Comput. Phys.* **1976**, *22*, 403.
- (5) Novstrup, K. A.; Travia, N. E.; Medvedev, G. A.; Stanciu, C.; Switzer, J. M.; Thomson, K. T.; Delgass, W. N.; Abu-Omar, M. M.; Caruthers, J. M. *J. Am. Chem. Soc.* **2010**, *132*, 558, Xiong, S.; Steelman, D. K.; Medvedev, G. A.; Delgass, W. N.; Abu-Omar, M. M.; Caruthers, J. M. *ACS Catalysis* **2014**, *4*, 1162.